Detecting order and chaos in three-dimensional Hamiltonian systems by geometrical methods

Yossi Ben Zion[1,2] and Lawrence Horwitz[1,2,3]
[1]*Department of Physics, Bar Ilan University, Ramat Gan 52900, Israel*
[2]*Department of Physics, Ariel University Center of Samarias, Ariel 44837, Israel*
[3]*School of Physics, Tel Aviv University, Ramat Aviv 69978, Israel*
(Received 25 June 2007; revised manuscript received 24 July 2007; published 23 October 2007)

We use a geometrical method to distinguish between ordered and chaotic motion in three-dimensional Hamiltonian systems. We show that this method gives results in agreement with the computation of Lyapunov characteristic exponents. We discuss some examples of unstable Hamiltonian systems in three dimensions, giving, as a particular illustration, detailed results for a potential obtained from a Hamiltonian obtained from a Yang-Mills system.

DOI: 10.1103/PhysRevE.76.046220 PACS number(s): 05.45.Gg, 45.20.Jj, 47.10.Df

I. INTRODUCTION

In the last decades much has been written about the criteria for chaotic motion in Hamiltonian systems [1–3]. The technique of surface of section (Poincaré plots) applied to detect chaotic behavior numerically has been very useful, particularly for two-dimensional Hamiltonian systems.

This method is also applicable in three dimensions [4] but it is difficult to apply as a criterion for unstable dynamics in this case [5]. For this case one may use the well-known Lyapunov characteristic exponents (LCEs). In the case of a Hamiltonian system with N degrees of freedom, the trajectories are characterized by N equal and opposite pairs of exponents. The character of the motion is determined by the maximal LCE (MLCE). The motion is considered to be chaotic if the MLCE is positive [3,6].

II. THEORY

A new method had recently been developed by Horwitz, Ben Zion, Lewkowicz, Schiffer, and Levitan (HBLSL) [7], based on the idea that the orbits are determined as geodesics on a dynamically induced surface. This method has some similarity to the use of the Jacobi metric (for which evolution is parametrized by the invariant action rather than the actual time t [7])—e.g, Szydlowski *et al.* [2], where the measure of the ratio of the region of negative curvature to the total volume of the physical region was also applied. With this comparative measure, we see that the HBLSL method provides not only the same condition on the parameter of nonintegrability as the MLCE, but also displays a very similar functional dependence on the parameter. The HBLSL method therefore contains information on chaotic behavior of the same nature as the MLCE.

The HBLSL method shows that the well-known characterization of chaotic Hamiltonian systems in terms of the curvature associated with a Riemannian metric tensor in the structure of the Hamiltonian can be extended to a wide class of potential models of standard form through the definition of a conformal metric [7]. This method induces a geometry on motion generated by the Hamilton equations with Hamiltonian of the form

$$H=\frac{\mathbf{p}^2}{2m}+V. \tag{1}$$

In particular, one starts with the Riemannian geometry of a metric space (which we call the *Gutzwiller manifold* [8]) for which the connection form follows from the Hamilton equations for a Hamiltonian of the form

$$H_G=\frac{1}{2m}g_{ij}p^ip^j, \tag{2}$$

where we have used the summation convention. Taking g_{ij} to be of the (conformal) form

$$g_{ij}=\frac{E}{E-V}\delta_{ij}, \tag{3}$$

we see that the two Hamiltonian forms (1) and (2) are equivalent on a given energy surface E. The geodesic equation obtained from the Hamiltonian (2) does not coincide with the structure of the Hamilton equations of motion associated with (1), but if the metric tensor (3) is used to raise the index of $\dot{x}_i$, one obtains

$$\ddot{x}^i=-M^i_{jk}\dot{x}^j\dot{x}^k, \tag{4}$$

where the new connection form, appropriate for the geodesics on an associated manifold $\{x^i\}$, is given by

$$M^{\ell}_{mn}\equiv\frac{1}{2}g^{\ell k}\frac{\partial g_{nm}}{\partial x^k}. \tag{5}$$

The manifold $\{x^i\}$, which we call the *Hamilton manifold*, has the property that in the special choice of coordinates for which the Hamiltonian has the form (1), and the definition (3) is used for the metric, the equations of motion (4) coincide with the Hamilton equations obtained from (1). We see that a geometrical structure has in this way been induced on the manifold $\{x^i\}$.

Let us consider the geodesic deviation

$$\xi^{\ell}=x'^{\ell}-x^{\ell} \tag{6}$$

between two nearby orbits (correlated by the time parameter t). The second-order geodesic deviation equations, from (4), are

 ©2007 The American Physical Society

$$\ddot{\xi}^\ell = -2M^\ell_{mn}\dot{x}^m\dot{\xi}^n - \frac{\partial M^\ell_{mn}}{\partial x^q}\dot{x}^m\dot{x}^n\xi^q. \quad (7)$$

Along the orbit $x^\ell(t)$ (almost common to x'^ℓ, x^ℓ), we define the covariant derivative

$$\frac{D_M \xi^\ell}{D_M t} = \dot{\xi}^\ell + M^\ell_{nm}\xi^m\dot{x}^n. \quad (8)$$

The second covariant derivative, together with Eq. (7), results in

$$\frac{D_M{}^2}{D_M t^2}\xi^\ell = R_M{}^\ell{}_{qmn}\dot{x}^q\dot{x}^n\xi^m, \quad (9)$$

where what we shall call the *dynamical curvature* is given by

$$R_M{}^\ell{}_{qmn} = \frac{\partial M^\ell_{qm}}{\partial x^n} - \frac{\partial M^\ell_{qn}}{\partial x^m} + M^k_{qm}M^\ell_{nk} - M^k_{qn}M^\ell_{mk}. \quad (10)$$

With the special form of the conformal metric, the dynamical curvature (10) can be written in terms of derivatives of the potential V and the geodesic equation (9) for the component of the deviation orthogonal to the velocity $v_i = \dot{x}_i$ becomes [7]

$$\frac{D^2_M P\boldsymbol{\xi}}{D_M t^2} = -P\mathcal{V}P\boldsymbol{\xi}, \quad (11)$$

where the matrix $\mathcal{V}$ is given by (ℓ, $i=1$, 2, 3 in three dimensions)

$$\mathcal{V}_{\ell i} = \left\{ \frac{3}{M^2 v^2}\frac{\partial V}{\partial x^\ell}\frac{\partial V}{\partial x^i} + \frac{1}{M}\frac{\partial^2 V}{\partial x^\ell \partial x^i} \right\} \quad (12)$$

and

$$P^{ij} = \delta^{ij} - \frac{v^i v^j}{\mathbf{v}^2}, \quad (13)$$

with $v^i \equiv \dot{x}^i$ defining a projection into a direction orthogonal to the velocity v^i.

Casetti *et al.* [9] have discussed cases for which, in their choice of metric and corresponding connection form, the curvature of the resulting manifold is positive and yet displays instability. Our choice of metric is somewhat different [10], and furthermore, as pointed out in [7], the stability criterion we use is based on a special connection form which emerges as applicable to the geodesic motion (what we have called a *dynamical connection form*), and its sign is not necessarily determined by the curvature of the full manifold defined by x^i (for which the connection form has torsion) [7].

The examples treated in [7] were for two-dimensional systems. It is important to verify that the HBLSL condition is also effective in three dimensions to establish the generality of the geometrical construction. To extend our previous analysis [7] to three dimensions, we express $\mathcal{V}$ in terms of its spectral resolution with eigenvalues λ_i,

$$\mathcal{V} = \sum_{i=1}^{3} \lambda_i u^{(i)} u^{(i)T}, \quad (14)$$

where the superscript T indicates transpose (adjoint for a real three-dimensional vector) and the $u^{(i)}$ are the eigenvectors. The scalar product

$$f^T P\mathcal{V}Pf = \sum_i \lambda_i (u^{(i)} f_\perp)^2 \quad (15)$$

for any three-dimensional vector f ($f_\perp$ is orthogonal to $\mathbf{v}$) is a convex linear form in the three eigenvalues, and therefore $P\mathcal{V}P$ has only positive eigenvalues if the λ_i are positive.

Instability should then occur if at least one of the eigenvalues of $\mathcal{V}$ is negative.

III. RESULTS AND DISCUSSION

One may easily verify that the three-dimensional oscillator potential is predicted to be stable. We now compare our results with the computation of Lyapunov exponents (MLCEs) for a family of three-dimensional systems.

We take for illustration here a generalization of the Yang-Mills potential

$$V = \frac{1}{2}(x^2y^2 + y^2z^2 + z^2x^2) + \alpha(x^4 + y^4 + z^4) \quad (16)$$

for $\alpha=0$. This is the Yang-Mills potential [5] which is chaotic.

For $\alpha=\frac{1}{4}$,

$$V = \frac{1}{4}(x^2 + y^2 + z^2)^2 = \frac{1}{4}r^4,$$

which is integrable.

We detect the behavior of the potential by two methods: the geometrical method and the MLCE.

Figure 1 shows the appearance of negative eigenvalues for energy $E=1$ and for several α indicates that the region of negative eigenvalues does not penetrate the physically accessible region for $\alpha < \frac{1}{12}$

We also calculate by the geometrical method with the same energy $E=1$ while α is varied from 0 (chaos) to $\frac{1}{4}$ (order) with a step of 10^{-3}. In Fig. 2 the solid blue line shows ρ vs α, where

$$\rho = \frac{\text{volume of region of negative eigenvalues}}{\text{volume of physically accessible region}}. \quad (17)$$

Any nonzero ρ indicates instability.

We also calculate MLCEs. We take the initial values to be the same for all α: $p_x=1$, $p_y=0.71$, $x=0.1$, $y=0.1$, and

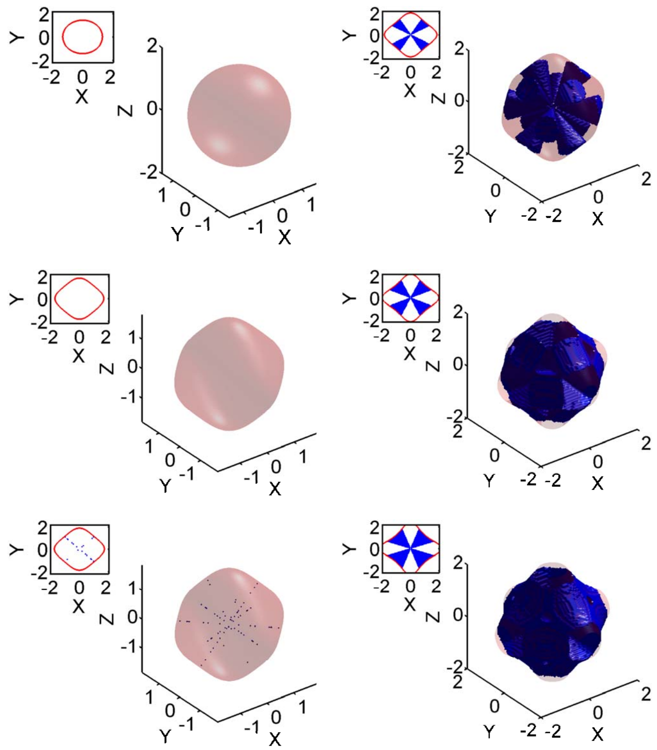

FIG. 1. (Color online) (a) corresponds to $\alpha=\frac{1}{4}$, for which the potential is spherically symmetric. The symmetry is broken in (b) with the choice $\alpha=\frac{1}{11}$, and negative eigenvalues appear in (c) ($\alpha\cong\alpha_c$). (d), (e), (f), correspond to of $\alpha=\frac{1}{16},\frac{1}{22},\frac{1}{32}$. The dark areas correspond to the existence of at least one negative eigenvalue. The figure at the upper left of each case shows a cut at $z=0$, where the boundaries are the limits of the physical region and the dark areas are regions of negative eigenvalues.

$z=0.1$. The value of p_z for a energy $E=1$ and for a given α is determined from Eq. (16).

In Fig. 2 the dashed green line shows the MLCE vs α for the same initial values and with the same step in α for $t=500$ time steps.

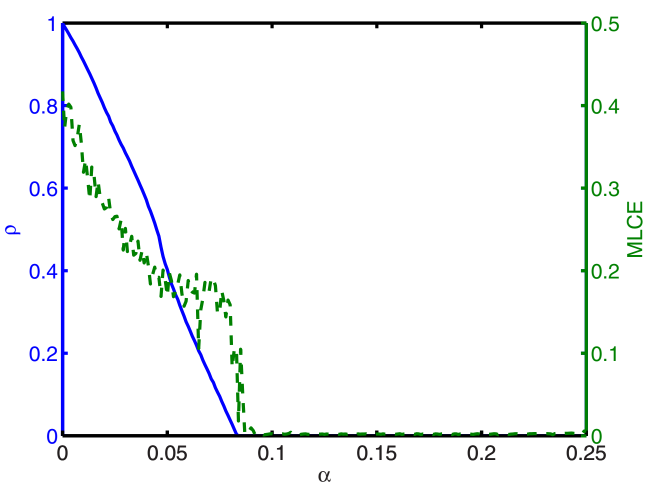

FIG. 2. (Color online) The solid blue line shows ρ [Eq. (17)] plotted as a function of α. The dashed green line shows MLCEs plotted as a function of α. The intercept is at $\alpha_c=0.084$.

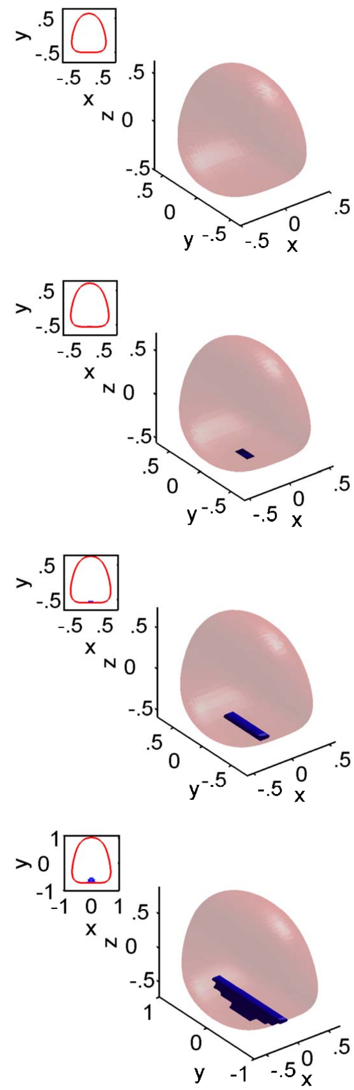

FIG. 3. (Color online) (a) corresponds to $E=0.2$, for which the Hamiltonian is stable. Negative eigenvalues appear in (b) ($E\cong E_c$). (c), (d) correspond to $E=0.3,0.5$. The dark areas correspond to the existence of at least one negative eigenvalue. The figure at the upper left of each case shows a cut at $y=0$, where the boundaries are the limits of the physical region and the dark areas are regions of negative eigenvalues.

The criteria for chaos determined by the geometrical method and by MLCE coincide for $\alpha<0.084$.

We also examine our criteria for a slight modification of the fifth-order expansion of a two-body Toda lattice Hamiltonian in three dimensions:

$$V=\frac{1}{2}(x^2+y^2+z^2)+x^2z-\frac{1}{3}z^3+\frac{3}{2}x^4+\frac{1}{2}z^4. \qquad (18)$$

Figure 3 shows the appearance of negative eigenvalues for several energies, indicating that the region of negative eigenvalues does not penetrate the physically accessible region for $E<0.24$. In Fig. 4 the solid blue line shows ρ vs E.

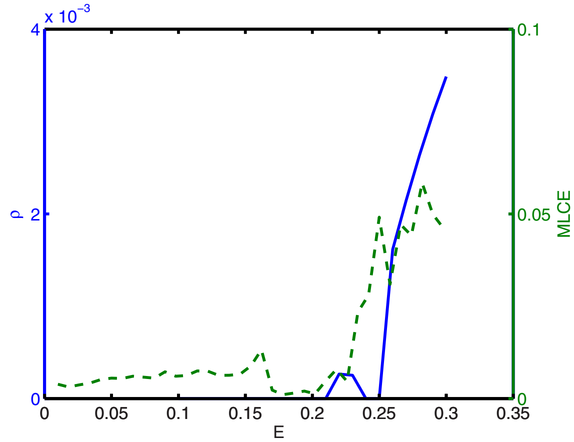

FIG. 4. (Color online) The solid blue line shows ρ [Eq. (17)] plotted as a function of E. The dashed green line shows MLCEs plotted as a function of E. The intercept is at $E_c = 0.24$.

The dashed green line shows MLCE vs E, indicating the same E_c. We take the initial values to be the same for all E: $p_x = 0.08$, $p_y = 0.08$, $x = 0.01$, $y = 0.01$, and $z = 0.01$. The value of p_z for a given E is determined from Eq. (18).

IV. CONCLUSION

We see that the HBLSL condition [7] is applicable for three-dimensional Hamiltonian systems and provides a sensitive test for both local and global (as for the MLCEs) instability. The MLCE computations for the examples we have treated here are much more laborious than the application of the HBLSL method, giving results in good agreement with the MLCEs.

The study of the three-dimensional case is important since our criteria provide conditions for local instability. The original work [7] does not provide a proof that the overall system will then behave in a chaotic way. That this instability creates a chaotic result emerges as a result of the computation. It is, in principle, possible that the effectiveness of the criteria that was seen in the two-dimensional examples was a result of the restricted topology of two dimensions; the three-dimensional computations show that they are effective in the more general case, which is therefore an important additional result.

ACKNOWLEDGMENT

We are grateful to Smadar Shatz for guidance on the computations.

[1] Lapo Casetti, Cecilia Clementi, and Marco Pettini, Phys. Rev. E **54**, 5969 (1996); P. Cipriani and M. Di Bari, Phys. Rev. Lett. **81**, 5532 (1998); Tetsuji Kawabe, Phys. Rev. E **71**, 017201 (2005).

[2] Marek Szydlowski and Adam Krawiec, Phys. Rev. D **53**, 6893 (1996); See also Marek Szydlowski and Jerzy Szczesny, *ibid.* **50**, 819 (1994); Marek Szydlowski and Adam Krawiec, *ibid.* **47**, 5323 (1993); M. Szydlowski and A. Lapeta, Phys. Lett. A **148**, 239 (1990).

[3] G. Benettin, L. Galgani, and J. M. Strelcyn, Phys. Rev. A **14**, 2338 (1976).

[4] M. Tabor, *Chaos and Integrability in Nonlinear Dynamics* (John Wiley and Sons, New York, (1989).

[5] W.-H. Steeb, J. A. Louw, and C. M. Villet, Phys. Rev. D **33**, 1174 (1986).

[6] A. Wolf, J. B. Swift, H. L. Swinney, and J. A. Vastano, Physica D **16**, 285 (1985).

[7] Lawrence Horwitz, Yossi Ben Zion, Meir Lewkowicz, Marcelo Schiffer, and Jacob Levitan, Phys. Rev. Lett. **98**, 234301 (2007).

[8] M. C. Gutzwiller, *Chaos in Classical and Quantum Mechanics* (Springer-Verlag, New York, (1990).

[9] L. Casetti, M. Pettini, and E. G. D. Cohen, Phys. Rep. **337**, 237 (2000).

[10] Casetti *et al.* state that "any system that reduces to a set of harmonic oscillators for sufficiently low energy behaves as a collection of harmonic oscillators do belong to this class." However, applying our method to a Hamiltonian with potential of the form $V = \frac{1}{2}(x^2 + y^2) + \frac{1}{6}(x^2 y^2)$, for the two-dimensional case, which lies in this category and leads to a positive curvature in their method, we obtain a clear signal of instability with our criterion based on the eigenvalues of Eq. (12), illustrating that there is an important difference between our criteria and those of [9].